energies

MDPI

Article

Combustion Characteristics of Methane Hydrate Flames

Yu-Chien Chien * and Derek Dunn-Rankin *

Department of Mechanical and Aerospace Engineering, University of California, Irvine, CA 92697, USA
* Correspondence: chieny@uci.edu (Y.-C.C.); ddunnran@uci.edu (D.D.-R.)

Received: 15 April 2019; Accepted: 8 May 2019; Published: 21 May 2019

Abstract: This research studies the structure of flames that use laboratory-produced methane hydrates as fuel, specifically for the purpose of identifying their key combustion characteristics. Combustion of a methane hydrate involves multiple phase changes, as large quantities of solid clathrate transform into fuel gas, water vapor, and liquid water during burning. With its unique and stable fuel energy storage capability, studies in combustion are focused on the potential usage of hydrates as an alternative fuel source or on their fire safety. Considering methane hydrate as a conventional combustion energy resource and studying hydrate combustion using canonical experimental configurations or methodology are challenges. This paper presents methane hydrate flame geometries from the time they can be ignited through their extinguishment. Ignition and burning behavior depend on the hydrate initial temperature and whether the clathrates are chunks or monolithic shapes. These behaviors are the subject of this research. Physical properties that affect methane hydrate in burning can include packing density, clathrate fraction, and surface area. Each of these modifies the time or the temperature needed to ignite the hydrate flames as well as their subsequent burning rate, thus every effort is made to keep consistent samples. Visualization methods used in combustion help identify flame characteristics, including pure flame images that give reaction zone size and shape and hydrate flame spectra to identify important species. The results help describe links between hydrate fuel characteristics and their resulting flames.

Keywords: methane hydrate; gas hydrate; methane clathrate; hydrate combustion; hydrate flame spectrum; hydrate ignition; watery flames

1. Introduction

Gas clathrate hydrates are ice-like crystalline compounds with guest molecules caged by non-stoichiometric hydrogen-bonded water [1]. Burning gas hydrates has been seen and demonstrated as a very interesting phenomenon for future energy and environmental benefit. For example, there are significant methane reserves stored in the form of methane clathrates in sediment in the ocean's continental shelves and in permafrost. Permafrost stores of hydrate are particularly vulnerable to warming trends, and significant methane releases from these regions have been noted in the past [2,3]. The potential combustion-related technological issues include safety during gas storage, using hydrates as in situ thermal sources for additional hydrate dissolution, and clean power because hydrates represent a unique fuel that is remarkably diluted (considering the water content) but still flammable. Gas hydrate research in combustion science and the demonstration of its potential merit are relatively scarce [4–8], though hydrate studies in general remain active in chemistry as well as in efforts for natural hydrate resource exploration (e.g., [9–12]).

Combustion of methane hydrates involves multiple phase changes (not conventional for a fuel), which adds new controlling dimensions to the physics and the chemistry of the combustion problem, and some recent studies that were originally motivated by clean energy demand have begun to unravel

some of the fundamental aspects of the direct combustion of methane hydrates. In some ways, the burning of a methane hydrate is similar to the devolatilization followed by volatiles combustion phases of coal burning [13]. That is, the first phase of coal combustion is the thermally-driven release of volatile hydrocarbons from the coal particle, which leaves behind the mineral and carbon-rich char. Similarly, thermally driven dissociation of hydrate releases volatile methane and leaves behind water. In both cases, the volatile combustible gas burns and produces the heat needed to continue the process. The difference is, of course, that the carbon-rich coal char is also combustible, whereas the residual water from hydrates is not. Nevertheless, the provision of energy to release sufficient volatiles that, when burning, contribute sufficient energy to maintain the subsequent release of flammable gas is the sequence necessary for continuous hydrate burning. Hence, in this paper, we describe the two important facets of the hydrate combustion process—ignition and steady burning of this unusual fuel.

Because the field is widely unexplored, even simple observations can contain important new information. For example, it can be seen from the hydrate combustion literature that the ignition for sustained burning must include a warming step to release sufficient methane gas to provide a robust flame capable of continued rapid hydrate dissociation. In addition, under nominally steady burning, it is observed from the literature (and from our experiments) that the hydrate flame color is different depending on the experiment. The current work provides a summary of gas hydrate burning, particularly focused on the ignition step and on flame visualization during hydrate combustion.

2. Materials and Methods

Artificial methane hydrate samples were created from ground ice solid phases with a 5.75 h heating cycle modified from Stern et al.'s standard hydrate formation procedure, operating around a peak pressure of 1500 psi [14]. The formation approach was to pressurize a sample of ice with methane gas and to then cycle the system across and through the hydrate equilibrium thermal boundary. Our ice-based hydrate samples were generally formed within a cylindrical mold that carried approximately 20 g of hydrate depending on the packing density for each operating condition. The production of reproducible (in terms of gas content and morphology) hydrate fuel samples is notoriously difficult, because hydrate formation depends on nucleation and growth behaviors at very small scales, thus extra care was taken to create reproducible samples. The process for making hydrates has already been extensively documented. Therefore, we only provided the skeleton of the process here. Nevertheless, it is important to recognize that even with carefully controlled conditions, hydrate internal structure can still vary in unpredictable ways. We therefore included sufficient repeat trials to ensure results with general applicability. The detailed procedure we used for producing the hydrate is documented in [15]. The hydrate formation literature has shown that the inclusion of sodium dodecyl sulfate (SDS), just at the ppm level, can promote hydrate growth rate, especially when forming hydrates from liquid [16–18]. We created ice-based hydrate samples with the addition of SDS in comparison to those with no SDS and compared them as they burned.

As mentioned in the introduction, the ignition process for hydrates is not trivial. This is because hydrates are thermodynamically unstable at room temperature and pressure, thus to stabilize the fuel long enough for it to be studied under burning conditions, the samples must first be chilled so that they do not spontaneously dissociate. This stabilizing procedure for us (and most others) involved quenching and storage in a liquid nitrogen cooled environment. Such procedures are standard in the hydrate research field [5,14], but the ultra-cold sample means that some warming is needed before the surface of the hydrate can release enough methane for ignition.

We conducted a series of hydrate ignition test experiments to understand this special solid fuel as it released cold flammable gases during dissociation in surroundings at room temperature and pressure. The first test allowed the cold hydrate sample temperature to rise on an aluminum foil base directly. One thermocouple was placed at the bottom of the aluminum foil and another was placed at 1 cm above the hydrate surface to monitor the temperature. The hydrate sample was ignited with a piezo ignitor and a butane flame lighter. The second test used an open-cup ignition apparatus and a

procedure with a butane lighter as the combustion initiator. This method was a simplified version of the American Society for Testing and Materials (ASTM) Cleveland open cup test for measuring the flash point for fuels [19]. Because hydrates exhibit two phase transitions and three phases, two thermocouples were installed. One was located at the bottom of the cup monitoring the hydrate temperature, and another was installed 3.8 cm from the cup bottom and above the height of the hydrate sample (1.25–2.5 cm).

When ignition was being evaluated, the conditions of the hydrate and the ignitor proximity were carefully monitored and recorded. When burning studies were the goal, such as during the overall spectral scan of the hydrate flame, we simply used a butane lighter to bathe the hydrate in heat for its start. The hydrate flame spectrum was then probed using a Princeton Instruments SpectraPro 2300i with a PIXIS 400 detector. The spectrometer was calibrated with a Xenon lamp. The flame images were recorded with a standard digital single-lens reflex (DSLR) camera.

3. Results

3.1. Ignition

The hydrate ignition tests were conducted with partially-crushed samples from originally cylindrically-shaped samples (see Figure 1) to allow more methane gas to release by providing a larger surface area exposed to the ambient environment. The hydrate samples were generally around 80% clathration ratio of methane, as referenced from the absolute maximum based on the total ideal hydrate cavity potential. The ideal hydrate (which was not ever achieved in practice) has a 0.15 methane to ice mass ratio, as compared to our experimental samples with a ratio of approximately 0.12. All hydrate samples were wrapped with aluminum foil and cooled with liquid nitrogen until they were ready for the desired tests. The laboratory room temperature was 23.8 °C ± 0.5.

Figure 1. A typical sample of methane hydrate while in the Teflon cylindrical mold.

Figure 2 shows the top view (~50 cm^2) and the side view of the initial ignition experiments. As is obvious, partially crushed hydrate samples varied in size and shape, but we found the behavior to be remarkably reproducible when the hydrate formation was reliable and the thermal conditions were controlled. The hydrate pile was approximately 3 cm tall. Both of the igniters were moving toward the hydrate sample with no physical contact during the process. The initial foil temperature was 2.3 °C, while the gas temperature was 22.5 °C. The hydrate samples could not be ignited with either the piezo igniter or the butane lighter in the first 60 s. The sample was too cold at this early time to release sufficient methane for flammability, though the methane inside the hydrate was dissociating with a distinct popping sound. At the 60 s time mark, the foil temperature read 16.4 °C, and the gas temperature was 23.7 °C. As the hydrate sample warmed up and the methane gas diffused slowly out of the sample, there was a distinct pattern of cold gas flowing down around the hydrate, as shown in Figure 3. The cold gases were flowing close to and along the foil, and they moved downward and away because of their relatively high density. The ignition by butane lighter of a steady flame occurred at the

89 s time mark, and at this time, the bottom side foil temperature was 18.5 °C. During ignition, the crushed powder hydrate region was the first spot lit into a methane flame, since the powder provided more methane volume and better air entrainment. Soon, a yellow methane flame was sustained out of the block shaped hydrate, including periodic rich methane jets, while a blue flame resided around the powder region with its more natural air admixing, as shown in Figure 4. Because the thermocouple located 10 mm above the sample was far away from the sample and measuring closed toward room temperature, it was measured at 23.0 °C at 2 mm above the hydrate sample at the point of ignition.

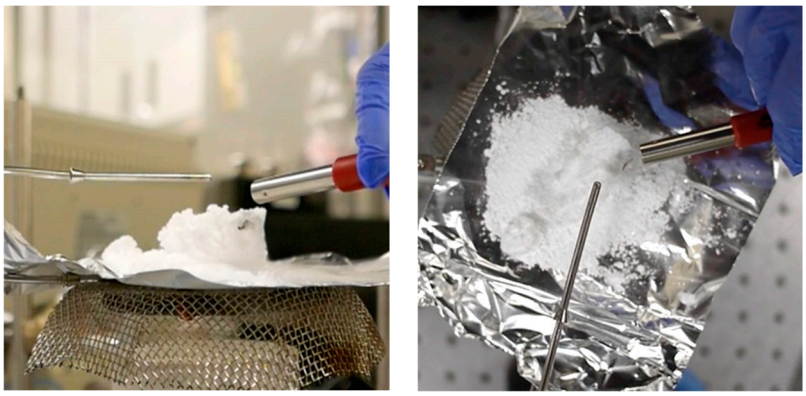

(**a**) (**b**)

Figure 2. Methane hydrate ignition tests in open air environment, (**a**) side view (**b**) top view.

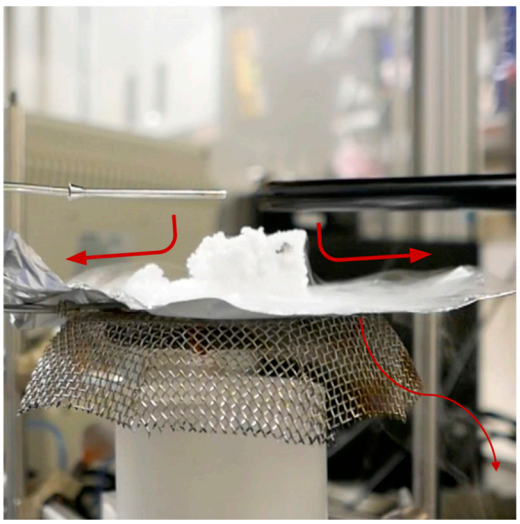

Figure 3. The methane hydrate warming up at room temperature. The arrows show the clear pathway of the cold gas flowing along the foil surface and moving downward. These flows were confirmed with both visual and schlieren imaging.

(**a**) (**b**)

Figure 4. The snapshot at the moment when the methane hydrate was ignited by a butane lighter. The bright yellow flame was from a methane jet releasing from the hydrate block, shown in (**a**), while a pale blue flame was distributed around the hydrate powder with more air admixing into the methane released from this section of the sample in (**b**).

There were several uncertainties observed from the ignition tests of methane hydrate exposed to open air. For example, the thermocouple situated above the sample was not able to provide enough information, and the ignition location varied with the format and the geometry of the hydrate sample being evaluated. It was clear that a more standard test would be preferable in order to identify the hydrate ignition conditions, particularly with its special properties. The second test format was a cup burner modeled after the configuration designed to evaluate the ignition of other condensed fuels. In this more standard approach, the hydrate sample was placed inside a stainless-steel cup with two thermocouples monitoring temperatures, as shown in Figure 5. One was at the bottom of the cup, while the second one was 3.8 cm from the bottom. The hydrate pile was 1.3–2.5 cm tall (from powder chunks to large blocks). The butane lighter was used to observe any flash point or ignition that occurred during the process. The cup opening was half-covered throughout the process. The ignition or the flash point was observed when the upper thermocouple averaged −3.8 °C for two tests (−3.3 and −4.3 °C), while the lower thermocouple measured the hydrate samples as averaging in temperatures at −64.5 °C (−62.6 and −65.5 °C). A completely open cup without any cover was also used for comparison, and in this case, the measured upper temperature was −4.7 °C and the hydrate temperature was −36.8 °C.

Figure 5. The cup ignition test with two thermocouples.

It should be noted that we recognize these ignition results are relatively sparse, but they are among the only attempts to quantify the characteristics of methane hydrate ignition. In addition, they reproducibly demonstrate the most important aspects of hydrate ignition that include a required minimum cake temperature, sufficient exposed surface area, and appropriate access to air for admixing. These elements are discussed more in later sections.

3.2. Burning

Figure 6 shows that, once burning, the flame had a distinct yellow-orange color when the samples included SDS. When SDS was not present, the flame had more of a blue-purple color around the gas hydrate with a stronger yellow color downstream. We presumed that the orange color arose from a sodium emission in the SDS case and that the yellow color in the post combustion zone could be nascent soot formation in the non-SDS hydrate. We also noted the foamy appearance in the case of the hydrate burning with SDS. We saw that excess amounts of SDS could make this foam a dominant feature that limited the hydrate combustion [6]. In order to compare the color and the character of the hydrate flame to one with similar characteristics of watery-fuel combustion but with the added feature that the flame be controllable (i.e., not affected by phase change processes), we developed a methane/air jet diffusion flame with varying amounts of water added to the methane. This gas-phase non-premixed flame simulated burning when water vapor naturally accompanied the fuel, as it did in a methane hydrate flame. Figure 7 shows a laminar methane diffusion jet flame as water was gradually added into the fuel to create a watery methane diffusion flame. The flame color changed from exhibiting a strong and brightly sooting region with no water addition to soot sitting on top of the flame tip as water was added. As even more water was added (up to the extinction limit), the flame color varied from blue to having a reddish hue. Based on these diffusion flame images, the formation of the blue-purple flame around the methane hydrate appeared related to the water vapor released into the flame. We expected that the water acted as a diluent to keep the flame temperature low and thereby avoid heavy sooting. To help confirm this feature, the gas hydrate optical spectrum was measured to identify the flame colors that appeared during combustion.

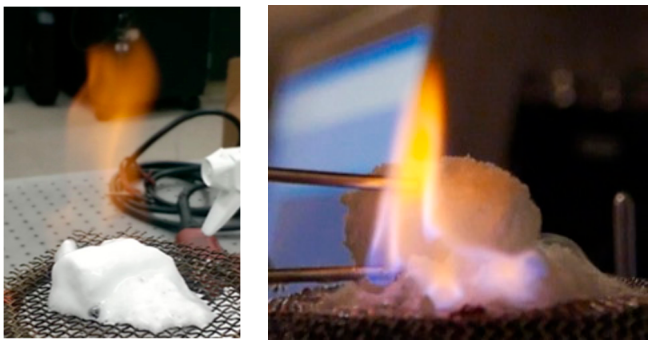

(**a**) (**b**)

Figure 6. Gas hydrate burning (**a**) with surfactant sodium dodecyl sulfate (SDS) and (**b**) with no surfactant.

Figure 7. Methane/air laminar jet diffusion flame. Jet diameter was 2 mm, and methane flow rate was 65 mL/min with air coflowing 1 L/min. The figure shows the evolution of the flame with water addition; (**a**) no water added; (**b**) 0.25 water/methane molar ratio; (**c**) 0.55 water/methane molar ratio; (**d**) flame at the extinction limit (0.57 water/methane molar ratio).

In order to determine the flame spectral character, the probe of the spectrometer was focused toward where the hydrate flame started, very close to the methane hydrate cake (around 4 cm height). The spectrometer had a 100 msec frame rate, and the results were averaged over 600 frames with background and noise subtraction. The amplitude of the signal changed between frames, but the spectral shape was very stable. The initial spectrum, Figure 8, showed one major peak located near 600 nm and two minor peaks between 400–450 nm and 500–550 nm.

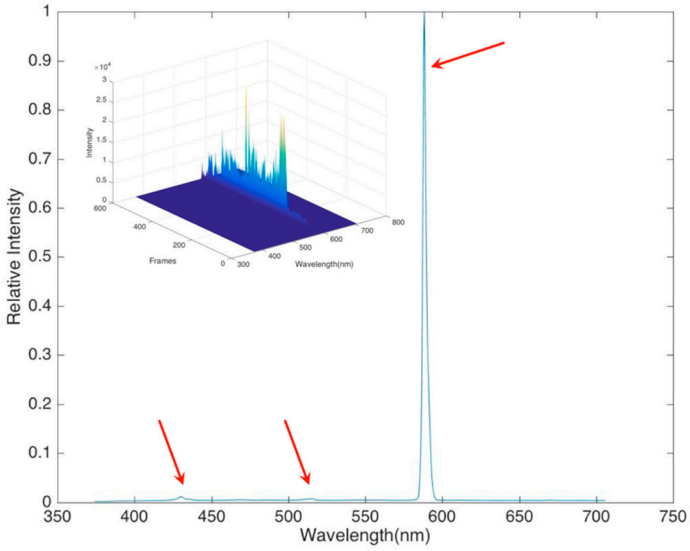

Figure 8. Gas hydrate spectrum over visible range; three peaks were found.

For a closer look, a different grating was used for the region close to 600 nm. With the higher resolution, two peaks were observed at 589.02 nm and 589.51 nm, as shown in Figure 9a. These two lines were clearly the sodium D line doublet (located at 589.0 and 589.6 nm). Over the 400–600 nm region, three peaks appeared—430.15 nm, 470.2 nm and 515.59 nm—which were the wavelength locations of the typical chemiluminescence species CH and C_2 in methane/air premixed flames [20–22], as shown in Figure 10. Perhaps unsurprisingly, the measured locations matched the three emission bands from the methane flames CH*(0,0), C_2*(1,0), and C_2*(0,0). Although these results were more confirmatory than exceptional, they did demonstrate that the spectral character of the flame was chemiluminescent and not strongly broadband, as would occur for soot. They also showed that the surfactants produced much of the strong color, and this was why the website images of methane hydrate combustion all had a strong orange-yellow coloring for dramatic presentation. A clean hydrate burning had much less luminosity and a pale blue color.

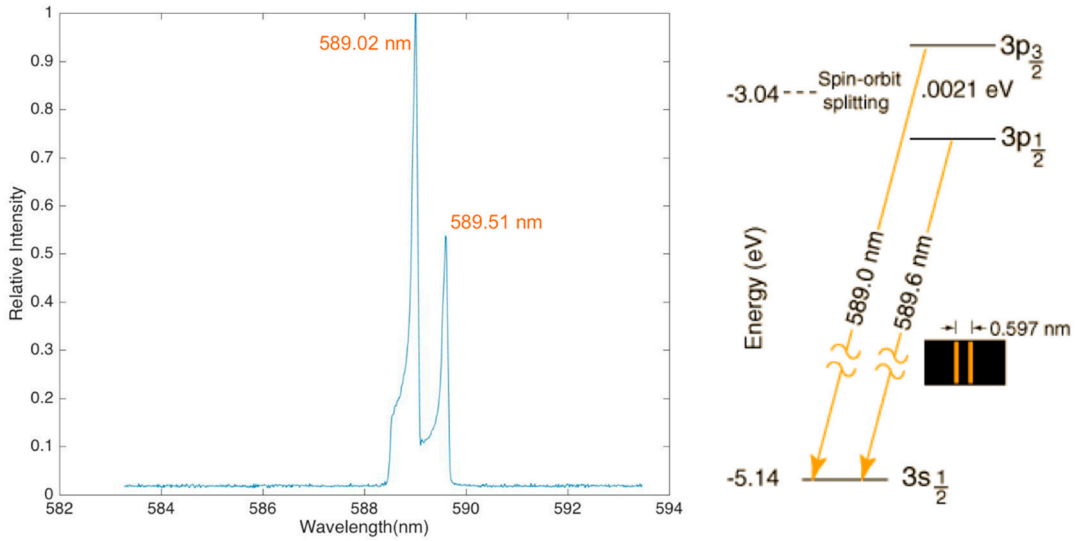

Figure 9. (**a**) Observed two peaks and (**b**) sodium D line doublet (courtesy of HyperPhysics from Georgia State University [23]).

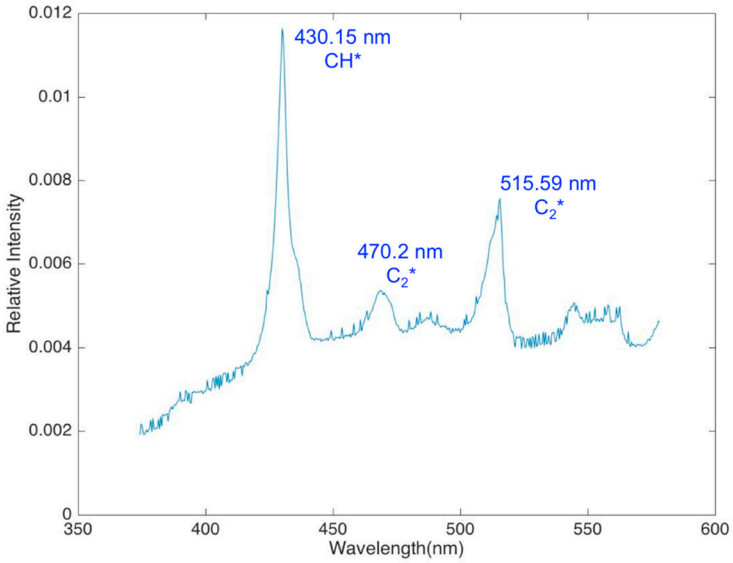

Figure 10. CH*(0,0), C2*(1,0), and C2*(0,0) emission bands of a methane hydrate flame.

4. Discussion

4.1. Ignition

Hydrate ignition is a complex process that is still not fully quantified. The results of this study show that stable burning requires that the sample reach some minimum temperature and that temperature can vary depending on the shape of the hydrate sample. Yoshioka et al. found that their cake temperature needed to reach −25 °C at the center for their spherical hydrates to burn steadily, and we found that temperatures of at least −4 °C are needed for steady burning of cylindrical cakes and powder piles. The reason for the minimum temperature is clear in that sufficient heat is needed from the flame to raise the hydrate temperature to dissociation at a rate sufficient to sustain the heat release needed for further dissociation. It seems that the cup burner is the most appropriate apparatus for determining hydrate ignition conditions.

4.2. Combustion

The spectral information during hydrate burning clearly shows the expected chemilumiscent emission and the influence of sodium from typical surfactants. The sodium line is also dominant in hydrates formed from salt water. We explored the use of sodium as a natural marker for temperature using a variant of the classic method of sodium line reversal [24]. Calibrating a tungsten lamp with varying input voltages against the blackbody emission measured from the filament provided a temperature/emission relationship. Then, using the lamp behind a hydrate flame, the voltage at which the lamp filament was just visible through the flame measured the hydrate flame's sodium temperature. The technique was promising but gave temperatures over 1900 K, which were higher than would be expected for a water diluted methane/air diffusion flame. The accurate measurement of hydrate flame temperature remains an experimental challenge we are pursuing with thin filament pyrometry (TFP). We measured the temperature of a methane flame fed by a melting hydrate [25], but thus far, there have been no temperature measurements of self-sustained natural hydrate flames.

In addition to the spectral information provided by the visual observation of the methane hydrate flames, there is also information contained in the time history of the total luminosity of the flame, as shown in the Figure 8 inset. The spectral measurements show that the proportion of the total flame luminosity arising from the different species remains nearly constant throughout the burn. That is, the flame color does not vary substantially in time. The total intensity, however, does vary as the flame fluctuates around the hydrate source. The buoyant flow driven by the rising hot gases also fluctuates, which gives a dynamic character to the flame. In the case of ideal spherical hydrate combustion [5], the flame fluctuation is clearly attributable to the growth of surface water that then drips from the base of the sphere, interrupting the flame anchor point and creating a fluctuation. In the case of our experiments, where the sample was more a distributed cake, the same effect of water could be observed, but it was not at a steady frequency, and thus the flame varied around the cake. A fast Fourier transform of the luminosity response showed one fairly dominant low frequency that arose from this buoyant plume shedding and water dripping frequency, and then a broader spectrum of frequency as the flame danced around the hydrate as methane was released.

5. Conclusions

This research examines the ignition and the burning of methane hydrates with particular attention to the repeatable tests for ignition and the evaluation of burning rates. Since this fuel is so unusual, the standard practices in combustion experiments required some modification and reformulation. Burning rates, for example, include the total mass loss from the sample but need to separate which part is water and which is fuel. For ignition, a standard condition is needed for self-sustained combustion that is different than typical ignition definitions, where there is not such a large residual heat capacity in the inert matrix. Biofuels, particularly wood, have some similarities in this regard, and thus we used ignition and burning concepts from that literature in our study.

The ignition studies in the cup burner format show that the hydrate ignited at the temperature around −65 °C, while the gas temperature above was −4 °C for the half-covered tests. This measurement required a detailed refinement in procedures, such as the amount of the hydrate samples, the location of the thermocouples, and especially the location of the igniter, which was needed to further define. Therefore, standardizing a preparation and ignition method for methane hydrates is important. The literature describes preparation of hydrates in a variety of ways that leaves a residual chill in the hydrate cake. This chill (often from storage in liquid nitrogen) means that the hydrate cake is supercooled. In this case, when the liquid water forms as the hydrate dissociates, it is possible that the cold core then freezes this water and blocks further fuel release, thereby quenching the flame. In naturally dissociating hydrates, this process is called self-healing [14]. For burning, once the hydrate core has reached a temperature that allows it to dissociate continuously, self-healing does not occur, but identifying if that temperature is independent of hydrate morphology and shape remains to be done.

We presented measurements of the visible optical spectrum of direct methane hydrates in combustion. A spectrometric evaluation identified the species responsible for the observed flame color. The strong sodium doublet is responsible for most of the orange/yellow coloration attributed to hydrate flame images in the literature and online. The pale blue flame zone is much more subtle and, as expected, this region arises from the three chemiluminescence bands, namely CH*(0,0), C_2*(1,0), and C_2*(0,0). These baseline experiments provide the starting point for future study where we will examine the color of hydrate flames when the hydrates are formed with different surfactants (including biologically derived rhamnolipids) and where they may contain other contaminants. For example, we may explore the color of flames around hydrates formed from fracking flowback water. We recognize that the work shared here is mostly qualitative in nature, but as the study of methane hydrate combustion is still very new and considering its potential as a future energy source and an unusual format in combustion, we see this discussion as an interesting contribution to a cleaner combustion future.

Author Contributions: Y.-C.C. conceived, designed, and carried out the experiments. She also compiled and analyzed the resulting data. D.D.-R. shared in conceptualization, in the discussion and analysis of the results, and contributed to the hypotheses presented. Y.-C.C. wrote the paper with assistance from co-author D.D.-R.

Funding: This research was funded by W. M. Keck Foundation, with project title Carbon-Free Deep-Ocean Power Science.

Acknowledgments: The authors appreciate the support of the W. M. Keck Foundation for gas hydrate research in the University of California, Irvine—Deep Ocean Power Science Laboratory. The authors appreciate the enthusiastic participation in experiments from Adrien Ruas and David Escofet-Martin.

Conflicts of Interest: The authors declare no conflict of interest.

References

1. Sloan, E.D., Jr. *Clathrate Hydrates of Natural Gases: Revised and Expanded*, 2nd ed.; CRC Press: Boca Raton, FL, USA, 1998; ISBN 978-0-8247-9937-3.
2. The, U.S. Geological Survey Gas Hydrates Project Climate. Available online: https://woodshole.er.usgs.gov/project-pages/hydrates/database.html (accessed on 13 March 2019).
3. Yin, Z.; Linga, P. Methane hydrates: A future clean energy resource. *Chin. J. Chem. Eng.* **2019**. [CrossRef]
4. Roshandell, M.; Santacana-Vall, J.; Karnani, S.; Botimer, J.; Taborek, P.; Dunn-Rankin, D. Burning Ice—Direct Combustion of Methane Clathrates. *Combust. Sci. Technol.* **2016**, *188*, 2137–2148. [CrossRef]
5. Yoshioka, T.; Yamamoto, Y.; Yokomori, T.; Ohmura, R.; Ueda, T. Experimental study on combustion of a methane hydrate sphere. *Exp. Fluids* **2015**, *56*, 192. [CrossRef]
6. Wu, F.-H.; Chao, Y.-C. A Study of Methane Hydrate Combustion Phenomenon Using a Cylindrical Porous Burner. *Combust. Sci. Technol.* **2016**, *188*, 1983–2002. [CrossRef]
7. Nakoryakov, V.E.; Misyura, S.Y.; Elistratov, S.L.; Manakov, A.Y.; Sizikov, A.A. Methane combustion in hydrate systems: Water-methane and water-methane-isopropanol. *J. Eng. Thermophys.* **2013**, *22*, 169–173. [CrossRef]
8. Nakoryakov, V.E.; Misyura, S.Y.; Elistratov, S.L.; Manakov, A.Y.; Shubnikov, A.E. Combustion of methane hydrates. *J. Eng. Thermophys.* **2013**, *22*, 87–92. [CrossRef]
9. Boswell, R.; Collett, T.S. Current perspectives on gas hydrate resources. *Energy Environ. Sci.* **2011**, *4*, 1206–1215. [CrossRef]
10. Koh, C.A.; Sum, A.K.; Sloan, E.D. State of the art: Natural gas hydrates as a natural resource. *J. Nat. Gas Sci. Eng.* **2012**, *8*, 132–138. [CrossRef]
11. Fujii, T.; Suzuki, K.; Takayama, T.; Tamaki, M.; Komatsu, Y.; Konno, Y.; Yoneda, J.; Yamamoto, K.; Nagao, J. Geological setting and characterization of a methane hydrate reservoir distributed at the first offshore production test site on the Daini-Atsumi Knoll in the eastern Nankai Trough, Japan. *Mar. Pet. Geol.* **2015**, *66*, 310–322. [CrossRef]
12. Li, J.; Ye, J.; Qin, X.; Qiu, H.; Wu, N.; Lu, H.; Xie, W.; Lu, J.; Peng, F.; Xu, Z.; et al. The first offshore natural gas hydrate production test in South China Sea. *China Geol.* **2018**, *1*, 5–16. [CrossRef]
13. Smoot, L.D.; Hedman, P.O.; Smith, P.J. Pulverized-coal combustion research at Brigham Young University. *Prog. Energy Combust. Sci.* **1984**, *10*, 359–441. [CrossRef]

14. Stern, L.A.; Circone, S.; Kirby, S.H.; Durham, W.B. Anomalous Preservation of Pure Methane Hydrate at 1 atm. *J. Phys. Chem. B* **2001**, *105*, 1756–1762. [CrossRef]
15. Biasioli, A. Methane Hydrate Growth and Morphology with Implications for Combustion. Master's Thesis, University of California, Irvine, CA, USA, 2015.
16. Zhong, Y.; Rogers, R.E. Surfactant effects on gas hydrate formation. *Chem. Eng. Sci.* **2000**, *55*, 4175–4187. [CrossRef]
17. Ganji, H.; Manteghian, M.; Sadaghiani zadeh, K.; Omidkhah, M.R.; Rahimi Mofrad, H. Effect of different surfactants on methane hydrate formation rate, stability and storage capacity. *Fuel* **2007**, *86*, 434–441. [CrossRef]
18. Botimer, J.D.; Dunn-Rankin, D.; Taborek, P. Evidence for immobile transitional state of water in methane clathrate hydrates grown from surfactant solutions. *Chem. Eng. Sci.* **2016**, *142*, 89–96. [CrossRef]
19. *Standard Test Method for Flash and Fire Points by Cleveland Open Cup Tester*; ASTM International: West Conshohocken, PA, USA, 2013.
20. Kojima, J.; Ikeda, Y.; Nakajima, T. Spatially Resolved Measurement of OH*, CH*, and C2* Chemiluminescence in the Reaction Zone of Laminar Methane/air Premixed Flames. *Proc. Combust. Inst.* **2000**, *28*, 1757–1764. [CrossRef]
21. Walsh, K.T.; Long, M.B.; Tanoff, M.A.; Smooke, M.D. Experimental and computational study of CH, CH*, and OH* in an axisymmetric laminar diffusion flame. *Symp. (Int.) Combust.* **1998**, *27*, 615–623. [CrossRef]
22. Dandy, D.S.; Vosen, S.R. Numerical and Experimental Studies of Hydroxyl Radical Chemiluminescence in Methane-Air Flames. *Combust. Sci. Technol.* **1992**, *82*, 131–150. [CrossRef]
23. Thornton, S.T.; Rex, A. *Modern Physics for Scientists and Engineers*; Cengage Learning: Boston, MA, USA, 2012; ISBN 978-1-133-71223-7.
24. Padilla, R.E.; Minniti, M.; Jaimes, D.; Garman, J.; Dunn-Rankin, D.; Pham, T.K. Thin Filament Pyrometry for Temperature Measurements in Fuel Hydrate Flames and Non-Premixed Water-Laden Methane-Air Flames. In Proceedings of the 8th National Combustion Meeting, Park City, UT, USA, 19–22 May 2013.
25. Wu, F.H.; Padilla, R.E.; Dunn-Rankin, D.; Chen, G.B.; Chao, Y.C. Thermal structure of methane hydrate fueled flames. *Proc. Combust. Inst.* **2017**, *36*, 4391–4398. [CrossRef]